Inorg. Chem. **2000,** *39,* 5796−5802

Syntheses and Structural Characterization of the (OC_nOPor) Capped Porphyrins: Co(OC_2OPor)·CH_2Cl_2, Co(OC_2OPor)(NO)$_{out}$·0.46$CHCl_3$, Co(OC_3OPor)·$CHCl_3$, and Co(OC_3OPor)(MeIm)·3C_7H_8

Paul G. Jene and James A. Ibers*

Department of Chemistry, Northwestern University, 2145 Sheridan Road, Evanston, Illinois 60208-3113

Received June 20, 2000

The compounds Co(OC_2OPor)·CH_2Cl_2 (**1**), Co(OC_2OPor)(NO)$_{out}$·0.46$CHCl_3$ (**2**), Co(OC_3OPor)·$CHCl_3$ (**3**), and Co(OC_3OPor)(MeIm)·3C_7H_8 (**4**) (OC_2OPor = 5,10,15,20-(benzene-1,2,4,5-tetrakis(2-phenyloxy)ethoxy)-$2',2'',2''',2''''$-tetraylporphyrinato dianion; OC_3OPor = 5,10,15,20-(benzene-1,2,4,5-tetrakis(2-phenyloxy)propoxy)-$2',2'',2''',2''''$-tetraylporphyrinato dianion; MeIm = 1-methylimidazole), have been synthesized, and their structures have been determined by single-crystal X-ray diffraction methods at $T = -120$ °C: **1**, $a = 8.824(1)$ Å, $b = 16.674(1)$ Å, $c = 16.836(1)$ Å, $\alpha = 104.453(1)°$, $\beta = 92.752(1)°$, $\gamma = 90.983(1)°$, $P\bar{1}$, $Z = 2$; **2**, $a = 9.019(1)$ Å, $b = 16.588(2)$ Å, $c = 16.909(2)$ Å, $\alpha = 103.923(2)°$, $\beta = 92.082(2)°$, $\gamma = 93.583(2)°$, $P\bar{1}$, $Z = 2$; **3**, $a = 13.484(3)$ Å, $b = 14.404(3)$ Å, $c = 14.570(3)$ Å, $\alpha = 105.508(3)°$, $\beta = 100.678(3)°$, $\gamma = 93.509(4)°$, $P\bar{1}$, $Z = 2$; **4**, $a = 16.490(1)$ Å, $b = 22.324(2)$ Å, $c = 17.257(1)$ Å, $b = 92.437(1)°$, $P2_1/n$, $Z = 4$. These compounds are the first structurally characterized Co-bound members of the OC_nOPor ligand system. The NO ligand in **2** and the MeIm ligand in **4** bind asymmetrically and lead to several metrical changes in these porphyrins, e.g., variations in average porphryin deviations and Co atom displacements relative to the porphyrinato N atoms and the mean porphyrin planes.

Introduction

For several decades porphyrin-based model systems of the heme active site have been used in an attempt to understand structure−function relationships in myoglobin (Mb) and hemoglobin (Hb).[1−6] A number of strategies have been employed to generate models that do not undergo irreversible oxidation and that mimic five-coordinate heme precursors. Models that can mimic the R- and T-states[7] of Hb are of particular interest. A plethora of elaborated porphyrins have been prepared, including "strapped",[8−14] "picnic basket",[15−19] "picket fence",[20−23] "pocket",[22,24,25] and "capped".[26−43] The number of structurally characterized model complexes continues to lag behind the

---

(1) Jameson, G. B.; Ibers, J. A. *Comments Inorg. Chem.* **1983**, *2*, 97−126.

(2) David, S.; Dolphin, D.; James, B. R. In *Frontiers in Bioinorganic Chemistry*; Xavier, A. V., Ed.; VCH: Weinheim, 1986; pp 163−182.

(3) Momenteau, M.; Reed, C. A. *Chem. Rev.* **1994**, *94*, 659−698.

(4) Jameson, G. B.; Ibers, J. A. In *Bioinorganic Chemistry*; Bertini, I., Gray, H. B., Lippard, S. J., Valentine, J. S., Eds.; University Science Books: Mill Valley, CA, 1994; pp 167−252.

(5) Springer, B. A.; Sligar, S. G.; Olson, J. S.; Phillips, G. N., Jr. *Chem. Rev.* **1994**, *94*, 699−714.

(6) Abbreviations used: TPP, 5,10,15,20-tetraphenylporphyrinato dianion; OC_2OPor, 5,10,15,20-(benzene-1,2,4,5-tetrakis(2-phenyloxy)ethoxy)-$2',2'',2''',2''''$-tetraylporphyrinato dianion; OC_3OPor, 5,10,15,20-(benzene-1,2,4,5-tetrakis(2-phenyloxy)propoxy)-$2',2'',2''',2''''$-tetraylporphyrinato dianion; Im, imidazole; MeIm, 1-methylimidazole; 1,2-Me_2Im, 1,2-dimethylimidazole; Hb, hemoglobin; Mb, myogoblin; C_n-cap ($n = 2−3$), TPP with linkages of the type $-OC_nO(CO)-$ connecting an ortho position on each of the phenyl rings to the 1,2,4,5 positions of the benzene cap; OEP, 2,3,7,8,12,13,17,18-octaethylporphyrin dianion; T(p-OCH_3)PP, TPP with $-OCH_3$ attached to the para positions of the four phenyl rings.

(7) Collman, J. P.; Reed, C. A. *J. Am. Chem. Soc.* **1973**, *95*, 2048−2049.

(8) Traylor, T. G.; Mitchell, M. J.; Tsuchiya, S.; Campbell, D. H.; Stynes, D. V.; Koga, N. *J. Am. Chem. Soc.* **1981**, *103*, 5234−5236.

(9) Baldwin, J. E.; Crossley, M. J.; Klose, T.; O'Rear, E. A., III.; Peters, M. K. *Tetrahedron* **1982**, *38*, 27−39.

(10) Ricard, L.; Fischer, J.; Weiss, R.; Momenteau, M. *Nouv. J. Chim.* **1984**, *8*, 639−642.

(11) Traylor, T. G.; Koga, N.; Deardurff, L. A.; Swepston, P. N.; Ibers, J. A. *J. Am. Chem. Soc.* **1984**, *106*, 5132−5143.

(12) Traylor, T. G.; Tsuchiya, S.; Campbell, D.; Mitchell, M.; Stynes, D.; Koga, N. *J. Am. Chem. Soc.* **1985**, *107*, 604−614.

(13) David, S.; Dolphin, D.; James, B. R.; Paine, J. B., III; Wijesekera, T. P.; Einstein, F. W. B.; Jones, T. *Can. J. Chem.* **1986**, *64*, 208−212.

(14) David, S.; James, B. R.; Dolphin, D.; Traylor, T. G.; Lopez, M. A. *J. Am. Chem. Soc.* **1994**, *116*, 6−14.

(15) Ricard, L.; Weiss, R.; Momenteau, M. *J. Chem. Soc., Chem. Commun.* **1986**, 818−820.

(16) Collman, J. P.; Brauman, J. I.; Fitzgerald, J. P.; Hampton, P. D.; Naruta, Y.; Sparapany, J. W.; Ibers, J. A. *J. Am. Chem. Soc.* **1988**, *110*, 3477−3486.

(17) Collman, J. P.; Brauman, J. I.; Fitzgerald, J. P.; Sparapany, J. W.; Ibers, J. A. *J. Am. Chem. Soc.* **1988**, *110*, 3486-3495.

(18) Schappacher, M.; Fischer, J.; Weiss, R. *Inorg. Chem.* **1989**, *28*, 389−390.

(19) Collman, J. P.; Zhang, X.; Wong, K.; Brauman, J. I. *J. Am. Chem. Soc.* **1994**, *116*, 6245−6251.

(20) Collman, J. P.; Gagne, R. R.; Reed, C. A.; Halbert, T. R.; Lang, G.; Robinson, W. T. *J. Am. Chem. Soc.* **1975**, *97*, 1427−1439.

(21) Collman, J. P.; Brauman, J. I.; Doxsee, K. M.; Halbert, T. R.; Suslick, K. S. *Proc. Natl. Acad. Sci. U.S.A.* **1978**, *75*, 564−568.

(22) Collman, J. P.; Brauman, J. I.; Iverson, B. L.; Sessler, J. L.; Morris, R. M.; Gibson, Q. H. *J. Am. Chem. Soc.* **1983**, *105*, 3052−3064.

(23) Wuenschell, G. E.; Tetreau, C.; Lavalette, D.; Reed, C. A. *J. Am. Chem. Soc.* **1992**, *114*, 3346−3355.

(24) Collman, J. P.; Brauman, J. I.; Collins, T. J.; Iverson, B.; Sessler, J. L. *J. Am. Chem. Soc.* **1981**, *103*, 2450−2452.

(25) Collman, J. P.; Brauman, J. I.; Collins, T. J.; Iverson, B. L.; Lang, G.; Pettman, R. B.; Sessler, J. L.; Walters, M. A. *J. Am. Chem. Soc.* **1983**, *105*, 3038−3052.

(26) Budge, J. R.; Ellis, P. E., Jr.; Jones, R. D.; Linard, J. E.; Szymanski, T.; Basolo, F.; Baldwin, J. E.; Dyer, R. L. *J. Am. Chem. Soc.* **1979**, *101*, 4762−4763.

(27) Almog, J.; Baldwin, J. E.; Crossley, M. J.; Debernardis, J. F.; Dyer, R. L.; Huff, J. R.; Peters, M. K. *Tetrahedron* **1981**, *37*, 3589−3601.

(28) Hashimoto, T.; Dyer, R. L.; Crossley, M. J.; Baldwin, J. E.; Basolo, F. *J. Am. Chem. Soc.* **1982**, *104*, 2101−2109.

10.1021/ic0006753 CCC: $19.00

number that have been characterized by other techniques.[3] The preparation and structural characterization of model complexes continues to play an important role in the study of these proteins.[44] In particular, the precise determination of metrical changes upon ligand binding to models provides important benchmarks for understanding structure−function relationships of ligand binding in heme proteins.

It has been known for some time that Co-substituted Mb and Hb exhibit reversible oxygen binding.[45] Simple compounds, e.g., Co(TPP)(NO),[46] have been used as isoelectronic models for ferrous dioxygen systems.[46] Also, Co substitution has been used to study other heme active sites, e.g., soluble guanylyl cyclase (sGC).[47] The sGC protein has not been structurally characterized, but it is known to contain a heme active site that binds NO. Reconstitution of this NO-activated protein with Co(heme) instead of Fe(heme) actually leads to an increase in activity.[47] Recently, fundamental questions regarding ligand binding effects in Co(porphyrin)(NO) systems[48,49] have been raised. There are relatively few structurally characterized Co-based model complexes compared with the many well-reviewed Fe-based models. Moreover, Co model systems offer advantages of stability over Fe model systems. These issues have led to a resurgence in the study of Co-substituted heme proteins[21,26,45,50−59] and related Co(porphyrin) systems.[19,48,57,60−74]

This paper reports the first four structurally characterized Co(OC$_n$OPor) complexes: Co(OC$_2$OPor)$\cdot$CH$_2$Cl$_2$ (**1**), Co(OC$_2$OPor)(NO)$_{out}\cdot$0.46CHCl$_3$ (**2**), Co(OC$_3$OPor)$\cdot$CHCl$_3$ (**3**), and Co(OC$_3$OPor)(MeIm)$\cdot$3C$_7$H$_8$ (**4**). Insofar as we know, only one other cobalt capped-porphyrin structure, Co(C$_3$-Cap),[75] is known, and only one other metalated OC$_2$OPor structure, Ru(OC$_2$OPor)(H$_2$O)$_{in}$(CO)$_{out}$,[34] is known. The present structures are free of crystallographically imposed symmetry that often results in disorder of the metal−ligand interactions in porphyrin systems. As a result, compounds **1**−**4** allow precise internal and comparative analysis of Co−ligand interactions.

Experimental Section

Materials and Equipment. All solvents and reagents were used as purchased, except CHCl$_3$, which was freshly distilled under N$_2$ from CaH$_2$; CH$_2$Cl$_2$, which was freshly distilled under N$_2$ from P$_2$O$_5$; and toluene, which was freshly distilled under N$_2$ from Na/benzophenone. Methyl alcohol, anhydrous 99.8% from Aldrich (packaged under N$_2$ in Sure/Seal bottles), was used for crystallizations. IR spectra were taken on a Bio-Rad FTS infrared spectrophotometer. Mass spectra were taken on a QUATTRO II electrospray mass spectrometer from Micromass, Altringham, England.

Porphyrin Metalation. Co was inserted into the free-base porphyrins by a modification of a literature method.[76] Co(CH$_3$CO$_2$)$_2\cdot$4H$_2$O (1.0 g) was refluxed in 25 mL of acetic acid, and 1−2 mL of the resultant solution was transferred to a refluxing solution of 5−10 mg of the porphyrin and 0.5 g of NEt$_4$Cl in 10 mL of acetic acid. The solution was refluxed for an additional 30 min. To the cooled solution was added 50 mL of CHCl$_3$. The solution was washed with 100 mL of H$_2$O, then with 50 mL of 5% Na$_2$CO$_3$(aq), filtered through a Na$_2$SO$_4$ cone, and dried on a rotary evaporator. The resultant Co(porphyrin) was stored under N$_2$.

---

(29) Shimizu, M.; Basolo, F.; Vallejo, M. N.; Baldwin, J. E. *Inorg. Chim. Acta* **1984**, *91*, 247−250.
(30) Garcia, B.; Lee, C.-H.; Blaskó, A.; Bruice, T. C. *J. Am. Chem. Soc.* **1991**, *113*, 8118−8126.
(31) Johnson, M. R.; Seok, W. K.; Ibers, J. A. *J. Am. Chem. Soc.* **1991**, *113*, 3998−4000.
(32) Kim, K.; Ibers, J. A. *J. Am. Chem. Soc.* **1991**, *113*, 6077−6081.
(33) Zhang, H.-Y.; Blaskó, A.; Yu, J.-Q.; Bruice, T. C. *J. Am. Chem. Soc.* **1992**, *114*, 6621−6630.
(34) Slebodnick, C.; Kim, K.; Ibers, J. A. *Inorg. Chem.* **1993**, *32*, 5338−5342.
(35) Ma, W.; Slebodnick, C.; Ibers, J. A. *J. Org. Chem.* **1993**, *58*, 6349−6353.
(36) Collman, J. P.; Zhang, X.; Herrmann, P. C.; Uffelman, E. S.; Boitrel, B.; Straumanis, A.; Brauman, J. I. *J. Am. Chem. Soc.* **1994**, *116*, 2681−2682.
(37) Lippard, S. J.; Berg, J. M. *Principles of Bioinorganic Chemistry*; University Science Books: Mill Valley, California, 1994.
(38) Ma, W.; Wilcoxen, K. M.; Szewczyk, J. W.; Ibers, J. A. *J. Org. Chem.* **1995**, *60*, 8081−8083.
(39) Slebodnick, C.; Fettinger, J. C.; Peterson, H. B.; Ibers, J. A. *J. Am. Chem. Soc.* **1996**, *118*, 3216−3224.
(40) Slebodnick, C.; Duval, M. L.; Ibers, J. A. *Inorg. Chem.* **1996**, *35*, 3607−3613.
(41) Johnson, M. R.; Seok, W. K.; Ma, W.; Slebodnick, C.; Wilcoxen, K. M.; Ibers, J. A. *J. Org. Chem.* **1996**, *61*, 3298−3303.
(42) Jene, P. G.; Chan, D. S.; Cooke, B. L.; Ibers, J. A. *Acta Crystallogr., Sect. C: Cryst. Struct. Commun.* **1999**, *55*, 801−806.
(43) Collman, J. P.; Fu, L. *Acc. Chem. Res.* **1999**, *32*, 455−463.
(44) Vojtechovsky, J.; Chu, K.; Berendzen, J.; Sweet, R. M.; Schlichting, I. *Biophys. J.* **1999**, *77*, 2153−2174.
(45) Hoffman, B. M.; Petering, D. H. *Proc. Natl. Acad. Sci. U.S.A.* **1970**, *67*, 637−643.
(46) Scheidt, W. R.; Hoard, J. L. *J. Am. Chem. Soc.* **1973**, *95*, 8281−8288.
(47) Dierks, E. A.; Hu, S.; Vogel, K. M.; Yu, A. E.; Spiro, T. G.; Burstyn, J. N. *J. Am. Chem. Soc.* **1997**, *119*, 7316−7323.
(48) Ellison, M. K.; Scheidt, W. R. *Inorg. Chem.* **1998**, *37*, 382−383.
(49) Scheidt, W. R.; Ellison, M. K. *Acc. Chem. Res.* **1999**, *32*, 350−359.
(50) Yonetani, T.; Yamamoto, H.; Erman, J. E.; Leigh, J. S., Jr.; Reed, G. H. *J. Biol. Chem.* **1972**, *247*, 2447−2455.
(51) Hoard, J. L.; Scheidt, W. R. *Proc. Natl. Acad. Sci. U.S.A.* **1973**, *70*, 3919−3922.
(52) Hori, H.; Ikeda-Saito, M.; Leigh, J. S., Jr.; Yonetani, T. *Biochemistry* **1982**, *21*, 1431−1437.
(53) Yu, N.-T.; Thompson, H. M.; Mizukami, H.; Gersonde, K. *Eur. J. Biochem.* **1986**, *159*, 129−132.
(54) Hu, S. *Inorg. Chem.* **1993**, *32*, 1081−1085.
(55) Kaminaka, S.; Zhou, Y.-X.; Tsuneshige, A.; Yonetani, T.; Kitagawa, T. *J. Am. Chem. Soc.* **1994**, *116*, 1683−1689.
(56) Miller, L. M.; Patel, M.; Chance, M. R. *J. Am. Chem. Soc.* **1996**, *118*, 4511−4517.
(57) Collman, J. P. *Inorg. Chem.* **1997**, *36*, 5145−5155.
(58) Kholodenko, Y.; Gooding, E. A.; Dou, Y.; Ikeda-Saito, M.; Hochstrasser, R. M. *Biochemistry* **1999**, *38*, 5918−5924.
(59) Marden, M. C.; Kiger, L.; Poyart, C.; Rashid, A. K.; Kister, J.; Stetzkowski-Marden, F.; Caron, G.; Haque, M.; Moens, L. *FEBS Lett.* **2000**, *472*, 221−224.
(60) Nishide, H.; Suzuki, T.; Nakagawa, R.; Tsuchida, E. *J. Am. Chem. Soc.* **1994**, *116*, 4503−4504.
(61) Cheng, S.-H.; Su, Y. O. *Inorg. Chem.* **1994**, *33*, 5847−5854.
(62) Scheidt, W. R.; Turowska-Tyrk, I. *Inorg. Chem.* **1994**, *33*, 1314−1318.
(63) Proniewicz, L. M.; Golus, J.; Nakamoto, K.; Kincaid, J. R. *J. Raman Spectrosc.* **1995**, *26*, 27−30.
(64) Morlino, E. A.; Walker, L. A., II; Sension, R. J.; Rodgers, M. A. J. *J. Am. Chem. Soc.* **1995**, *117*, 4429−4430.
(65) Morlino, E. A.; Rodgers, M. A. J. *J. Am. Chem. Soc.* **1996**, *118*, 11798−11804.
(66) Richter-Addo, G. B.; Hodge, S. J.; Yi, G.-B.; Khan, M. A.; Ma, T.; Caemelbecke, E. V.; Guo, N.; Kadish, K. M. *Inorg. Chem.* **1996**, *35*, 6530−6538.
(67) Schmidt, E.; Zhang, H.; Chang, C. K.; Babcock, G. T.; Oertling, W. A. *J. Am. Chem. Soc.* **1996**, *118*, 2954−2961.
(68) Kini, A. D.; Washington, J.; Kubiak, C. P.; Morimoto, B. H. *Inorg. Chem.* **1996**, *35*, 6904−6906.
(69) Salzmann, R.; Ziegler, C. J.; Godbout, N.; McMahon, M. T.; Suslick, K. S.; Oldfield, E. *J. Am. Chem. Soc.* **1998**, *120*, 11323−11334.
(70) Owens, J. W.; Perry, M.; Seybert, D. W. *Inorg. Chim. Acta* **1998**, *277*, 1−7.
(71) Zavarine, I. S.; Kini, A. D.; Morimoto, B. H.; Kubiak, C. P. *J. Phys. Chem. B* **1998**, *102*, 7287−7292.
(72) Godbout, N.; Sanders, L. K.; Salzmann, R.; Havlin, R. H.; Wojdelski, M.; Oldfield, E. *J. Am. Chem. Soc.* **1999**, *121*, 3829−3844.
(73) Van Doorslaer, S.; Bachmann, R.; Schweiger, A. *J. Phys. Chem. A* **1999**, *103*, 5446−5455.
(74) Kadish, K. M.; Ou, Z.; Tan, X.; Boschi, T.; Monti, D.; Fares, V.; Tagliatesta, P. *J. Chem. Soc., Dalton* **1999**, 1595−1601.
(75) Sparapany, J. W.; Crossley, M. J.; Baldwin, J. E.; Ibers, J. A. *J. Am. Chem. Soc.* **1988**, *110*, 4559−4564.
(76) Adler, A. D.; Longo, F. R.; Kampas, F.; Kim, J. *J. Inorg. Nucl. Chem.* **1970**, *32*, 2443−2445.

Table 1. Selected Crystallographic Data

	Co(OC$_2$OPor)·CH$_2$Cl$_2$ (**1**)	Co(OC$_2$OPor)(NO)out·0.46CHCl$_3$ (**2**)	Co(OC$_3$OPor)·CHCl$_3$ (**3**)	Co(OC$_3$OPor)(MeIm)·3C$_7$H$_8$ (**4**)
formula	$C_{58}H_{42}N_4O_8Co \cdot CH_2Cl_2$	$C_{58}H_{42}N_5O_9Co \cdot 0.46CHCl_3$	$C_{62}H_{50}N_4O_8Co \cdot CHCl_3$	$C_{66}H_{56}N_6O_8Co \cdot 3C_7H_8$
fw	1066.81	1067.58	1157.36	1396.5
space group	$P\bar{1}$	$P\bar{1}$	$P\bar{1}$	$P2_1/n$
a, Å	8.824(1)	9.019(1)	13.484(3)	16.490(1)
b, Å	16.674(1)	16.588(2)	14.404(3)	22.324(2)
c, Å	16.836(1)	16.909(2)	14.570(3)	17.257(1)
α, deg	104.453(1)	103.923(2)	105.508(3)	90
β, deg	92.752(1)	92.082(2)	100.678(3)	92.437(1)
γ, deg	90.983(1)	93.583(2)	93.509(4)	90
V, Å^3	2394.8(2)	2447.4(5)	2661.3(9)	6346.8(9)
Z	2	2	2	4
ρ_{calc} g/cm^3	1.479	1.449	1.444	1.461
μ, cm^{-1}	5.4	5.0	5.4	3.4
T, °C	−120	−120	−120	−120
$R(F)^a$	0.041	0.082	0.069	0.082
$R_w(F^2)^b$	0.113	0.196	0.145	0.160

^{a} $R(F) = (\sum|F_o| - |F_c|)/\sum|F_o|$. ^{b} $R_w(F_o^2) = [\sum[w(F_o^2 - F_c^2)^2]/\sum wF_o^4]^{1/2}$; $w^{-1} = \sigma^2(F_o^2) + (0.04F_o^2)^2$ for $F_o^2 > 0$; $w^{-1} = \sigma^2(F_o^2)$ for $F_o^2 \leq 0$.

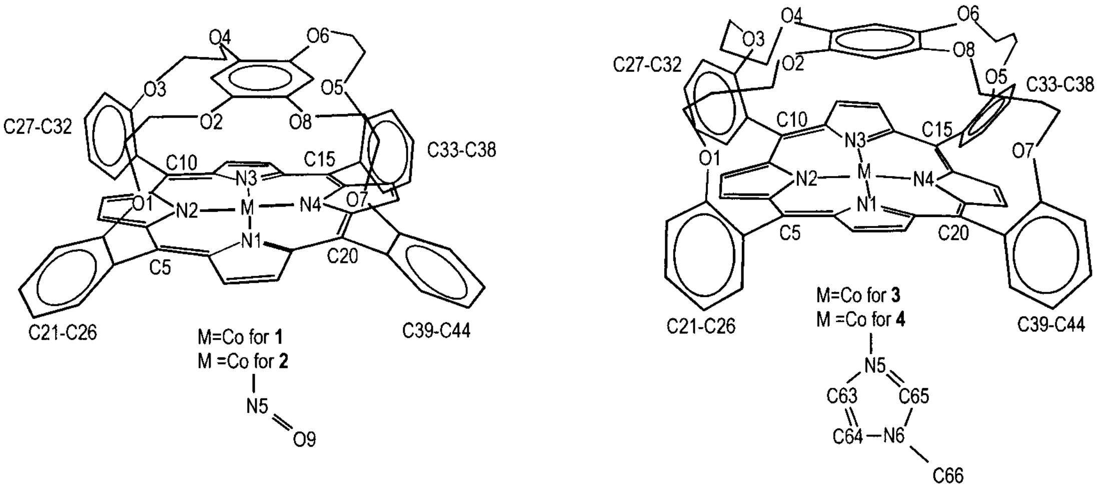

Figure 1. Labeling schemes for Co(OC$_2$OPor)·CH$_2$Cl$_2$ (**1**), Co(OC$_2$OPor)(NO)$_{out}$·0.46CHCl$_3$ (**2**), Co(OC$_3$OPor)·CHCl$_3$ (**3**), and Co(OC$_3$OPor)(MeIm)·3C$_7$H$_8$ (**4**).

Synthesis of Co(OC$_2$OPor)·CH$_2$Cl$_2$ (1). H$_2$(OC$_2$OPor) was prepared following the literature method,[41] and it was recrystallized from CH$_2$Cl$_2$/CH$_3$OH. Co was inserted, and then crystals of **1** were grown by slow diffusion of CH$_3$OH (~4 mL) into a CH$_2$Cl$_2$ solution of **1** (~4 mg) at −20 °C. Low-resolution mass spectrum (ES): *m*/*z* 980.5 [Co(OC$_2$OPor)]$^+$ (100%).

Synthesis of Co(OC$_2$OPor)(NO)$_{out}$·0.46CHCl$_3$ (2). With the use of air-free techniques, Co(OC$_2$OPor) (~5 mg) was dissolved in 1.5 mL of CHCl$_3$. Excess 1,2-Me$_2$Im was added. NO(g) was bubbled into the solution for 10 min.[77] Then 0.65 mL of solution was transferred to a Schlenk diffusion tube by gastight syringe, where it was layered with CH$_3$OH (~5 mL) and stored at −20 °C. Crystals of **2** formed over 1 month. Low-resolution mass spectrum (ES): *m*/*z* 1018.1 [Co(OC$_2$OPor)(NO)]$^+$ (15%) and 980.6 [Co(OC$_2$OPor)]$^+$ (100%). IR (KBr, cm^{-1}): ν_{NO} = 1667. ***CAUTION**: NO is toxic, and reactions should be performed in a well-ventilated fume hood.*

Synthesis of Co(OC$_3$OPor)·CHCl$_3$ (3). H$_2$(OC$_3$OPor) was prepared following the literature method,[35] and it was recrystallized from CHCl$_3$/CH$_3$OH. Co was inserted, and crystals of **3** were grown by slow diffusion of CH$_3$OH (~4 mL) into a CHCl$_3$ solution of **3** (~4 mg) at −20 °C. Low-resolution mass spectrum (ES): *m*/*z* 1037 [Co(OC$_3$OPor)]$^+$ (100%).

Synthesis of Co(OC$_3$OPor)(MeIm)·3C$_7$H$_8$ (4). Co(OC$_3$OPor)·CHCl$_3$ (~5 mg) was dissolved in 0.9 mL of toluene. Then 20 μL of MeIm was added. The solution was transferred to a Schlenk diffusion tube by gastight syringe and layered with ~6 mL of hexane. The tube was sealed under N$_2$ and stored at 25 °C. Crystals of **4** formed in 2 weeks. Low-resolution mass spectrum (ES): *m*/*z* 1036 [Co(OC$_3$OPor)]$^+$ (100%) and *m*/*z* 980.6 [(OC$_3$OPor)]$^+$ (80%).

X-ray Crystal Structure Determinations. A chosen crystal was attached with silicone cement to the tip of a drawn glass fiber on a goniometer head and transferred to the cold stream of a Bruker Smart 1000 CCD diffractometer. The crystal was kept at −120 °C for the length of the data collection. For all four structures, data were collected with 0.3° ω scans for 10, 2, 15, or 30 s/frame for **1**, **2**, **3**, or **4**, respectively. Final unit cell parameters were determined from a global refinement of the positions of all reflections having $I > 10\sigma(I)$, as performed by the processing program SAINT+.[78] No absorption correction was applied to compound **2**. A face-indexed absorption correction was applied to **1**, **3**, and **4** with the use of XPREP.[79] Then the program SADABS,[78] which relies on redundancy in the data, was used to apply some semiempirical corrections for frame variations and other effects to all four compounds. The structures were solved with the use of the direct methods program SHELXS of the SHELXTL PC suite of programs.[79] The structures were refined by full-matrix least-squares techniques with the program SHELXL.[79] For all four structures all non-hydrogen atoms were modeled anisotropically, except the chloroform C atom, C59, of compound **2,** which was refined isotro-

---

(77) Scheidt, W. R.; Frisse, M. E. *J. Am. Chem. Soc.* **1975**, *97*, 17−21.

(78) SMART Version 5.054 Data Collection and SAINT-Plus Version 6.02A Data Processing Software for the SMART System; Bruker Analytical X-Ray Instruments, Inc., Madison, WI, 2000.

(79) Sheldrick, G. M. SHELXTL DOS/Windows/NT Version 5.10; Bruker Analytical X-Ray Instruments, Inc., Madison, WI, 1997.

Table 2. Selected Bond Lengths (Å) and Angles (deg) for Co(OC$_2$OPor)·CH$_2$Cl$_2$ (**1**), Co(OC$_2$OPor)(NO)$_{out}$·0.46CHCl$_3$ (**2**), Co(OC$_3$OPor)·CHCl$_3$ (**3**), and Co(OC$_3$OPor)(MeIm)·3C$_7$H$_8$ (**4**)

	(**1**)	(**2**)	(**3**)	(**4**)
Co−N1	1.962(2)	1.970(4)	1.957(4)	1.985(3)
Co−N2	1.968(2)	1.990(3)	1.938(4)	1.993(3)
Co−N3	1.964(2)	1.958(4)	1.957(4)	1.988(3)
Co−N4	1.966(2)	1.973(3)	1.946(4)	1.976(3)
av Co−N$_{eq}$[a]	1.965(1)	1.972(7)	1.949(5)	1.985(4)
av N−C$_a$	1.384(2)	1.383(2)	1.387(4)	1.380(4)
av C$_a$−C$_b$	1.433(2)	1.435(4)	1.432(3)	1.439(2)
av C$_a$−C$_m$	1.386(2)	1.389(6)	1.383(2)	1.388(3)
N1−Co−N2	90.11(6)	90.03(13)	90.34(16)	89.69(12)
N1−Co−N3	176.52(6)	173.56(14)	174.28(17)	172.31(12)
N1−Co−N4	89.78(6)	89.24(14)	90.29(16)	89.96(12)
N2−Co−N3	90.00(6)	88.85(13)	90.15(16)	89.96(12)
N2−Co−N4	178.92(6)	169.59(14)	171.56(17)	173.76(12)
N3−Co−N4	90.17(6)	90.71(14)	90.06(16)	89.56(12)
C21−C26 dihedral[b]	64.7(1)	68.1(1)	57.3(1)	64.2(1)
C27−C32 dihedral	78.0(1)	76.0(1)	86.2(1)	70.7(1)
C33−C38 dihedral	70.8(1)	79.5(1)	63.4(1)	82.2(1)
C39−C44 dihedral	62.0(1)	61.2(1)	65.8(1)	76.4(1)

[a] The standard deviation is that of the mean. In some instances, for example Co−N$_{eq}$ for **2**, there are significant differences among quantities averaged and the entry is only given for comparative purposes. [b] Measured as the dihedral angle between the 6-atom mean plane of the phenyl ring and the 24-atom mean plane of the porphyrin. C$_a$, C$_b$, and C$_m$ stand respectively for the α and *β* pyrrole carbon atoms, and methine carbon atoms. N$_{eq}$ stands for the porphyrinato nitrogen atoms N1, N2, N3, and N4.

Table 3. Displacements[a] (Å) from the 24-Atom Porphyrin Mean Plane

	1	**2**	**3**	**4**
Co[b]	−0.019(2)	0.161(3)	0.036(4)	0.133(3)
N1	0.029(2)	0.047(3)	0.067(4)	−0.027(3)
N2	−0.028(2)	−0.006(3)	−0.122(4)	0.009(3)
N3	0.052(2)	0.055(3)	0.129(4)	0.027(3)
N4	−0.048(2)	−0.032(3)	−0.092(4)	0.042(3)
C1	0.064(2)	0.062(4)	0.269(5)	−0.038(4)
C2	0.224(2)	0.209(4)	0.520(5)	−0.137(4)
C3	0.252(2)	0.253(4)	0.473(5)	−0.152(4)
C4	0.109(2)	0.136(4)	0.222(5)	−0.065(4)
C5	0.034(2)	0.074(4)	−0.0671(5)	0.018(4)
C6	−0.036(2)	−0.014(4)	−0.305(5)	0.053(4)
C7	−0.151(2)	−0.167(4)	−0.544(5)	0.123(4)
C8	−0.233(2)	−0.268(4)	−0.499(5)	0.103(4)
C9	−0.152(2)	−0.161(4)	−0.183(5)	0.033(4)
C10	−0.157(2)	−0.185(4)	0.085(5)	−0.002(4)
C11	0.028(2)	0.005(4)	0.292(5)	−0.038(4)
C12	0.192(2)	0.172(4)	0.533(5)	−0.131(4)
C13	0.302(2)	0.315(4)	0.472(5)	−0.128(4)
C14	0.178(2)	0.190(4)	0.190(5)	−0.022(4)
C15	0.087(2)	0.151(4)	−0.085(5)	−0.002(4)
C16	−0.064(2)	−0.038(4)	−0.280(5)	0.029(4)
C17	−0.222(2)	−0.228(4)	−0.549(5)	0.050(4)
C18	−0.278(2)	−0.328(4)	−0.481(5)	0.096(4)
C19	−0.138(2)	−0.164(4)	−0.183(5)	0.090(4)
C20	−0.047(2)	−0.078(4)	0.067(5)	0.068(4)
av[c]	0.129	0.160	0.282	0.062

[a] Here and in succeeding tables a positive displacement is away from the benzene cap for compounds **1**−**4** (and toward the ligand for **2** and **4**). [b] Not involved in the calculation of the mean plane. [c] Average deviation from the 24-atom porphyrin core.

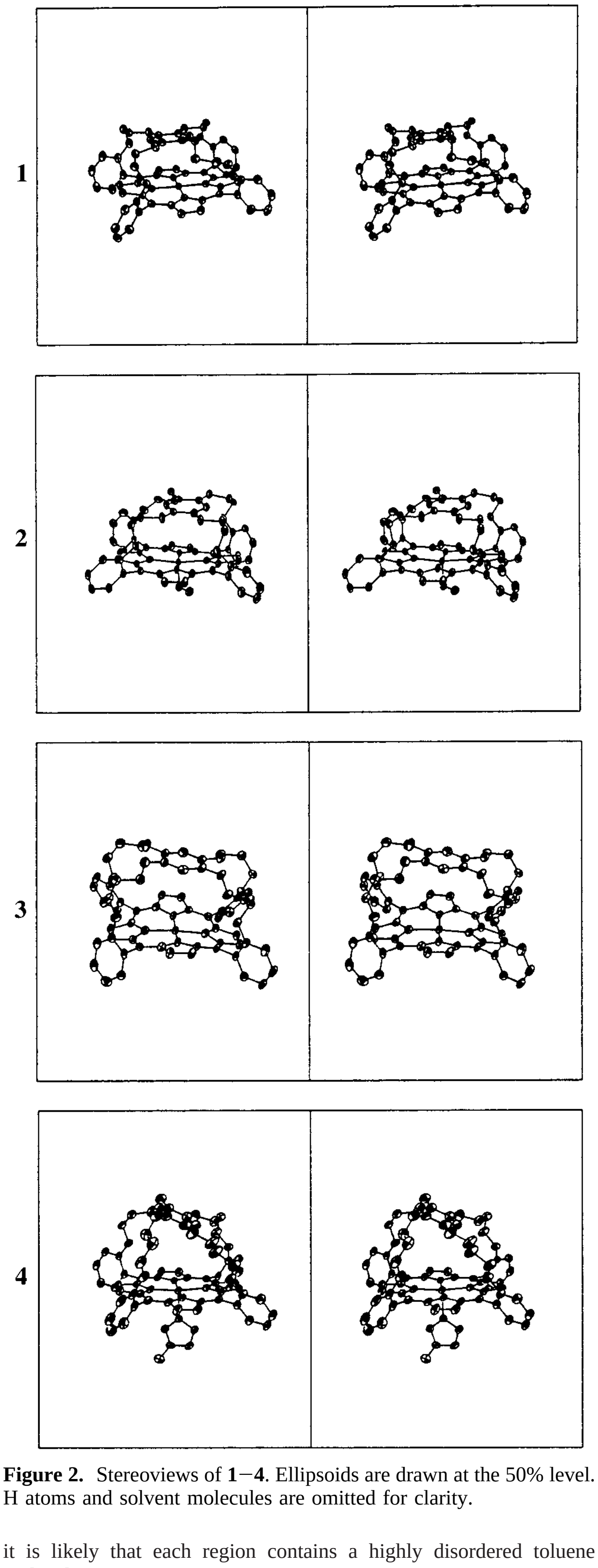

Figure 2. Stereoviews of **1**−**4**. Ellipsoids are drawn at the 50% level. H atoms and solvent molecules are omitted for clarity.

pically. Hydrogen atoms were placed at calculated positions and refined with a riding model.

The refinements of **1**−**3** were straightforward. The occupancy of the chloroform site in **2** refined to an occupancy of 0.464(4). However, for **4** there were difficulties in refining solvent(s) of crystallization, as only one toluene could be resolved. Electron density associated with two 210 Å^3 potential solvent regions, each containing 47 electrons, was identified and removed with the SQUEEZE[80] algorithm in the PLATON[81] suite of programs. From these volumes and electron counts, it is likely that each region contains a highly disordered toluene molecule.

Crystallographic details for the four compounds may be found in Table 1. Additional information is available in the Supporting Informa-

---

(80) van der Sluis, P.; Spek, A. L. *Acta Crystallogr., Sect. A: Found. Crystallogr.* **1990**, *46*, 194−201.

(81) Spek, A. L. *Acta Crystallogr., Sect. A: Found. Crystallogr.* **1990**, *46*, C34.

Table 4. Comparison of Structural Parameters among (OC_nOPor) Porphyrins

structure	av dev[a](Å)	ΔM (Å)[b]	displacement of cap (Å) vertical	displacement of cap (Å) lateral	dihedral angle of cap (deg)	*T* (°C)	ref
$H_2(OC_2OPor)\cdot$acetic acid	0.10		3.81	0.54	8.0	−115(2)	31
$H_2(OC_2OPor)\cdot CH_2Cl_2$	0.09		3.80	0.54	7.3	−163(2)	83
$Co(OC_2OPor)\cdot CH_2Cl_2$ (**1**)	0.13	−0.02	3.78	0.56	7.2	−120(2)	this work
$Co(OC_2OPor)(NO)_{out}\cdot 0.46CHCl_3$ (**2**)	0.16	0.16	3.94	0.55	7.6	−120(2)	this work
$Ru(OC_2OPor)(H_2O)_{in}(CO)_{out}$	0.06	0.26	4.80	0.60	8	−167(2)	34
$H_2(OC_3OPor)$	0.07		4.74	0.54	14.3	−167(2)	40
$Co(OC_3OPor)\cdot CHCl_3$ (**3**)	0.28	0.04	4.51	1.02	4.6	−120(2)	this work
$Co(OC_3OPor)(MeIm)\cdot 3C_7H_8$ (**4**)	0.06	0.13	5.27	0.27	23.1	−120(2)	this work
$Fe(OC_3OPor)(Cl)$	0.15	0.52	4.65	1.35	3.9	−167(2)	40
$Fe(OC_3OPor)(CO)(MeIm)$	0.08	0.06	5.55	0.21	20.3	−167(2)	40
$Fe(OC_3OPor)(CO)(1,2\text{-}Me_2Im)$	0.07	0.10	5.59	0.66	5.3	−167(2)	40

[a] Average deviation from the mean plane through the 24 atoms of the porphryin core (N1−N4 and C1−C20). [b]Displacement of the metal from the mean plane.

tion. Drawings of the molecular structures of the porphyrinic portions of **1**−**4** are presented in Figure 1, and stereoviews are presented in Figure 2.

Results and Discussion

$Co(OC_2OPor)\cdot CH_2Cl_2$ (1) and $Co(OC_2OPor)(NO)_{out}\cdot 0.46CHCl_3$ (2). Note that, despite the presence of excess 1,2-Me_2Im in the reaction mixture, compound **2**, a five-coordinate nitrosyl complex, is the sole product. There are no reported six-coordinate Co(Por)(NO)(base) structures, where base is an imidazole. It appears that NO can displace 1,2-Me_2Im, a sterically hindered nitrogenous base, in elaborated Co(Por) systems, in agreement with some observations on heme systems[82] and the idea that NO binding to the Co-substituted heme site of sGC can trigger cleavage of the histidine bonds.[47]

The crystal structures of both $Co(OC_2OPor)\cdot CH_2Cl_2$ (**1**) and $Co(OC_2OPor)(NO)_{out}\cdot 0.46CHCl_3$ (**2**) consist of the packing of one porphyrin molecule with an ordered solvent molecule (one CH_2Cl_2 molecule in **1** and 0.46 $CHCl_3$ molecule in **2**) in the asymmetric unit. The benzene cap of **1** and **2** consists of a 1,2,4,5-substituted benzene cap connected by four-atom linkages of the type $-O(CH_2)_2O-$ to the ortho positions of the phenyl rings of 5,10,15,20-tetraphenylporphyrin. Compound **1** is unligated, whereas compound **2** has NO bound on the sterically unhindered face of the porphyrin. The similarity of unit cell contents and volumes implies no unusual differences in packing, despite the differences in solvation. Hence these two structures provide an excellent opportunity to examine the structural changes to $Co(OC_2OPor)\cdot CH_2Cl_2$ upon NO binding.

In $Co(OC_2OPor)\cdot CH_2Cl_2$ (**1**) the Co center is coordinated symmetrically to the four N_{eq} atoms, with Co−N_{eq} distances ranging from 1.962(3) to 1.968(2) Å (Table 2). The Co atom is −0.019(2) Å out of the mean 24-atom porphyrin plane (Table 3) in the direction of the cap. Upon ligation by NO, the Co atom in $Co(OC_2OPor)(NO)_{out}\cdot 0.46CHCl_3$ (**2**), now five-coordinate, moves 0.161(3) Å out of the mean porphyrin plane in the direction of the NO ligand. But the Co atom in **2** is not symmetrically disposed with respect to the N_{eq} atoms, as the Co−N_{eq} distances range from 1.958(4) to 1.990(3) Å. Other individual and averaged bond lengths seem unaffected by NO binding. The 24-atom porphyrin plane in both compounds is saddle shaped, but is more distorted in compound **2**, as reflected in a 0.031 Å increase in average deviation. The dihedral angles of the phenyl groups are similar in the two structures.

Three structures containing OC_2OPor have been structurally characterized previously (Table 4). Two of these are different solvates of $H_2(OC_2OPor)$,[31,83] and the other is $Ru(OC_2OPor)(H_2O)_{in}(CO)_{out}$.[34] The metrical details for $H_2(OC_2OPor)$ are in good agreement, despite the different solvents of crystallization. Among the five OC_2OPor structures, lateral displacement of the cap shows little variation, differing by only 0.06 Å between the most extreme values. In contrast, average deviation of the 24-atom plane seems metal dependent, with compounds **1** and **2** exhibiting greater average deviation than $H_2(OC_2OPor)$, and $Ru(OC_2OPor)(H_2O)_{in}(CO)_{out}$[34] exhibiting less deviation. Vertical displacement of the cap is obviously affected by ligand binding, especially by binding under the cap. Thus, $Ru(OC_2OPor)(H_2O)_{in}(CO)_{out}$[34] shows the greatest increase in vertical displacement, ∼1 Å, relative to $H_2(OC_2OPor)$. But for unknown reasons the displacement for compound **2**, which has the NO ligand on the unhindered face, is 0.16 Å greater than that in compound **1**. The tilt of the cap relative to the porphyrin plane seems unaffected by metalation or ligand binding.

Table 5. Selected Bond Lengths (Å) and Angles (deg) for Porphyrins **2** and **4**

	2	**4**
Co−L_{ax}[a]	1.837(4)	2.132(3)
angle between Co1−L_{ax} and the porphyrin plane normal	2.1	2.6
ligand orientation[b]	134.1	74.9
L_{ax} to 24-atom mean plane	89.3	85.9
N1−Co−L_{ax}	94.25(17)	91.99(12)
N2−Co−L_{ax}	92.20(16)	93.31(12)
N3−Co−L_{ax}	92.20(16)	95.70(12)
N4−Co−Lax[a]	93.78(14)	92.93(12)

[a] L_{ax} = N (of NO) for **2** and N(of MeIm) for **4**. [b]Measured as the angle between the Co−N−O plane and the N1−N3 vector for **2** and the N5−N6, C63−C65 plane and N1−N3 vector for **4**.

Table 5 lists additional metrical details of the ligands bound to compounds **2** and **4**. For compound **2**, the NO ligand exhibits asymmetry in its binding. The Co−N(NO) vector, rather than being normal to the mean porphyrin plane, is 2.1° off-axis with the ligand tilted slightly toward atoms N2 and N3. This small deviation would certainly go undetected if a crystallographic rotation axis through the metal atom were present, as is often the case with metalloporphyrin crystal structures. Atom O9 of the nitrosyl ligand is oriented almost directly toward one of the phenyl rings (C33−C38), with a closest calculated nonbonded contact of 2.80 Å for H34A···O9.

Table 6 provides comparisons among other five-coordinate Co porphyrin nitrosyl complexes. Discounting Co(TPP),[46] whose structure suffers from crystallographically imposed symmetry that makes the resolution of the NO atoms imprecise, bond

---

(82) Traylor, T. G.; Sharma, V. S. *Biochemistry* **1992**, *31*, 2847−2849.

(83) Jene, P. G.; Ibers, J. A. Unpublished results.

Table 6. Selected Five-Coordinate Cobalt Porphyrin Nitrosyls

complex	M−N$_{eq}$^{a} (Å)	M−N$_{NO}$ (Å)	∠MNO (deg)	N−O (Å)	ΔM^b(Å)	ν_{NO} (cm^{-1})	T (°C)	ref
Co(OC_2OPor)(NO)$_{out}$· 0.46$CHCl_3$ (**2**)	1.958(4), 1.970(4), 1.973(3), 1.990(3)	1.837(4)	121.8(3)	1.174(4)	0.16	1667^c	−120(2)	this work
Co(OEP)(NO)	1.977(1), 1.977(1), 1.989(1), 1.994(1)	1.8444(9)	122.70(8)	1.1642(13)	0.16	1677^d	−143(2)	48
Co(TPP)(NO)	1.978(4)	1.833(53)	∼135	1.01(2)	0.09	1689^c	−45(2)	46
Co(T(*p*-OCH_3)PP)(NO)	1.837(3), 2.128(4)	1.854(5)	119.6(45)	1.195(8)	0.20	1696^c	−20(1)	66

^{a} Symmetry independent Co−N(Por) bonds. ^{b} Displacement of the Co atom from the 24-atom mean porphyrin plane. ^{c} KBr pellet. ^{d} Nujol mull.

lengths, angles, and IR frequencies are generally in good agreement among these porphyrins. The asymmetry of axial ligands in Co[48,49] (Table 6) and Fe[49,84] five-coordinate porphyrin nitrosyls has been commented on recently. The asymmetry found in Co(T(*p*-OCH_3)PP)(NO),[66] seems excessive.

Co(OC_3OPor)·$CHCl_3$ (3) and Co(OC_3OPor)(MeIm)·3C_7H_8 (4). The crystal structures of both Co(OC_3OPor)·$CHCl_3$ (**3**) and Co(OC_3OPor)(MeIm)·3C_7H_8 (**4**) consist of the packing of one porphyrin molecule and one (compound **3**) or three (compound **4**) solvent molecules in the asymmetric unit. In **4**, two of the three toluene solvent molecules are badly disordered. The linkage between benzene cap and porphyrin in these structures is −O(CH_2)$_3$O−. Compound **4** can be considered as a model for deoxyCoMb or R-state deoxyCoHb.

Compound **3** is unligated, whereas compound **4** has MeIm bound on the sterically unhindered face of the porphyrin. Upon ligation of MeIm the average Co−N$_{eq}$ bond length increases by 0.036(5) Å, but in contrast to ligation of Co(OC_2OPor)·CH_2Cl_2 by NO all Co−N$_p$ bonds lengthen. Other average bond lengths are essentially unchanged. The Co atom, which is not symmetrically positioned in either compound **3** or **4**, shifts from slightly closer to atom N2 to slightly closer to atom N4. The N1−Co−N3 bond angle decreases by 2.0(2)°, but the N2−Co−N4 bond angle increases by 2.2(2)°, implying that the N$_p$ atoms follow the Co atom out of the mean porphyrin plane. This is supported by the N atom displacements in Table 3. The Co atom moves from 0.036(4) to 0.133(3) Å out of the mean porphyrin plane toward the MeIm ligand. This is a smaller displacement than that seen in compound **2**, despite the fact that MeIm is a bulkier ligand than NO.

Average distortions of the 24-atom mean planes for compounds **3** and **4** also display a pattern different from that in compounds **1** and **2** (Table 3). Compound **3** has the largest average deviation of the known OC_nOPor structures, whereas compound **4** has the smallest. This variation is opposite to that of **1** and **2**, and certainly differs from the pattern of Fe(OC_3OPor)(CO)(base) species in Table 4. Among the (OC_3OPor)-based structures, cap dihedral angles and lateral displacement of the cap do not seem to be related to metalation or ligand binding. This suggests that the cap superstructure is flexibly attached to the porphyrin core, and likely has only a limited impact on mean deviations of the (OC_3OPor)-based porphyrins. Of course the maximum vertical displacement of the cap is correlated with ligand binding under the cap. The two carbonyl species have vertical cap displacements that are 0.28−1.08 Å greater than those of the other (OC_3OPor)-based porphyrins.

Both compounds **3** and **4** show saddle distortions (Table 3), but the maximum deviations are three to four times larger in compound **3**. This is visible in the stereoviews of Figure 2. The cap superstructure in these compounds is flexible, and the 18.5° change in cap tilt between **3** and **4** probably results simply from differences in crystal packing, although it is not possible to comment further given the solvent disorder in compound **4**. In the solid state the flexibility of the porphyrin core, as manifested in its various modes of distortion, has been well documented.[62,85−89] In some instances, for example Ni(OEP)[90−92] and Fe(OEP),[89] polymorphs exist that show pronounced structural differences. In addition, subtle crystal packing effects, as engendered for example by solvate molecules, can bring about profound structural changes in a given porphyrin system. Interest in the role ligands play in porphyrin distortions has generated predictive rules for the TPP and OEP systems.[69,72,93] But the relative importance of crystal packing forces, solvents of crystallization, and ligand binding on the conformational variations in the (OC_3OPor) system remain unclear.

Comparisons of compound **4** with other unligated CoMb model complexes and a recent unligated Mb protein structure are presented in Table 7. Among the models, the Co−N$_{eq}$ bond length average differs by a maximum of 0.03(1) Å, the Co−N$_{MeIm}$ bond length differs by a maximum of 0.025(3) Å, and the ΔCo displacements are equal. This excellent agreement among the unconstrained[94,95] models and compound **4** suggests that the cap superstructure has minimal effect on MeIm coordination. An important corollary is that differences in six-coordinate ligand binding between unconstrained models and (OC_3OPor)(MeIm)-based models can reasonably be assigned to ligand−cap interactions.

---

(84) Ellison, M. K.; Scheidt, W. R. *J. Am. Chem. Soc.* **1997**, *119*, 7404−7405.

(85) Munro, O. Q.; Bradley, J. C.; Hancock, R. D.; Marques, H. M.; Marsicano, F.; Wade, P. W. *J. Am. Chem. Soc.* **1992**, *114*, 7218−7230.

(86) Sparks, L. D.; Medforth, C. J.; Park, M.-S.; Chamberlain, J. R.; Ondrias, M. R.; Senge, M. O.; Smith, K. M.; Shelnutt, J. A. *J. Am. Chem. Soc.* **1993**, *115*, 581−592.

(87) Barkigia, K. M.; Renner, M. W.; Furenlid, L. R.; Medforth, C. J.; Smith, K. M.; Fajer, J. *J. Am. Chem. Soc.* **1993**, *115*, 3627−3635.

(88) Jentzen, W.; Simpson, M. C.; Hobbs, J. D.; Song, X.; Ema, T.; Nelson, N. Y.; Medforth, C. J.; Smith, K. M.; Veyrat, M.; Mazzanti, M.; Ramasseul, R.; Marchon, J.-C.; Takeuchi, T.; Goddard, W. A., III; Shelnutt, J. A. *J. Am. Chem. Soc.* **1995**, *117*, 11085−11097.

(89) Neal, T. J.; Cheng, B.; Ma, J.-G.; Shelnutt, J. A.; Schulz, C. E.; Scheidt, W. R. *Inorg. Chim. Acta* **1999**, *291*, 49−59.

(90) Meyer, E. F., Jr. *Acta Crystallogr., Sect. B: Struct. Crystallogr. Cryst. Chem.* **1972**, *28*, 2162−2167.

(91) Cullen, D. L.; Meyer, E. F., Jr. *J. Am. Chem. Soc.* **1974**, *96*, 2095−2102.

(92) Brennan, T. D.; Scheidt, W. R.; Shelnutt, J. A. *J. Am. Chem. Soc.* **1988**, *110*, 3919−2924.

(93) Salzmann, R.; McMahon, M. T.; Godbout, N.; Sanders, L. K.; Wojdelski, M.; Oldfield, E. *J. Am. Chem. Soc.* **1999**, *121*, 3818−3828.

(94) Scheidt, W. R. *J. Am. Chem. Soc.* **1974**, *96*, 90−94.

(95) Little, R. G.; Ibers, J. A. *J. Am. Chem. Soc.* **1974**, *96*, 4452−4463.

Table 7. Comparison of Selected Co(Por)(MeIm) Species with Mb

complex	$M-N_{eq}$[a] (Å)	$M-N_{(MeIm)}$ (Å)	ΔM[b] (Å)	MeIm angle (deg)	MeIm tilt (deg)[c]	*T* (°C)	ref
$Co(OC_3OPor)(MeIm\cdot 3C_7H_8$ (**4**)	1.985(6)	2.132(3)	0.13	74.9	2.6	−120(2)	this work
Co(OEP)(MeIm)	1.96(1)	2.15(1)	0.13	10	1	presumed 25(2)	95
Co(TPP)(MeIm)	1.977(3)	2.157(3)	0.13	∼45	7.2	20(1)	94
unligated ferrous Mb	2.07(3)	2.14(2)	0.39	not reported	5.8	−163	44

[a] Average of the metal porphyrinato N atom bonds. [b] Displacement of the metal from the 24-atom mean porphyrin plane. [c] Measured as the angle between the metal−N(MeIm) or metal−N(histidine) bond and the normal to the mean porphyrin plane.

Table 7 provides an interesting comparison of the accuracy obtainable in modern studies of the Mb system versus that in model systems. It seems clear that structural studies of model systems, even if such systems are not functional models for Mb and Hb, remain important as one means to probe structure−function relationships in the hemoproteins.

Acknowledgment. This research was supported by National Institutes of Health Grant HL 13157 and an IMGIP fellowship. Funds for the purchase of the Micromass Quattro II triple quadrupole electrospray mass spectrometer were provided through NIH Grant S10 RR11320.

Supporting Information Available: Crystallographic files, in CIF format, for $Co(OC_2OPor)\cdot CH_2Cl_2$ (**1**), $Co(OC_2OPor)(NO)_{out}\cdot 0.46CHCl_3$ (**2**), $Co(OC_3OPor)\cdot CHCl_3$ (**3**), and $Co(OC_3OPor)(MeIm)\cdot 3C_7H_8$ (**4**). This material is available free of charge via the Internet at http://pubs.acs.org.

IC0006753